Use of *ade1* mutation for development of a versatile red/white color assay of amyloid-induced oxidative stress in *Saccharomyces cerevisiae*

Vidhya Bharathi M J

A Dissertation Submitted to

Indian Institute of Technology Hyderabad

In Partial Fulfillment of the Requirements for

The Degree of Master of Technology

भारतीय प्रौद्योगिकी संस्थान हैदराबाद
Indian Institute of Technology Hyderabad

Department of Biotechnology

June, 2016

Declaration

I declare that this written submission represents my ideas in my own words, and where others' ideas or words have been included, I have adequately cited and referenced the original sources. I also declare that I have adhered to all principles of academic honesty and integrity and have not misrepresented or fabricated or falsified any idea/data/fact/source in my submission. I understand that any violation of the above will be a cause for disciplinary action by the Institute and can also evoke penal action from the sources that have thus not been properly cited, or from whom proper permission has not been taken when needed.

Vidhya Bharathi M J

BO14MTECH11008

Approval Sheet

This thesis entitled Use of *ade1* mutation for development of a versatile red/white color assay of amyloid-induced oxidative stress in *Saccharomyces cerevisiae* by Vidhya Bharathi M J is approved for the degree of Master of Technology from IIT Hyderabad.

Dr. Basant Kumar Patel

(Thesis advisor)

Department of Biotechnology

IIT Hyderabad

Dr. Rajkumara Eerappa

Department of Biotechnology

IIT Hyderabad

Dr. Anamika Bhargava

Department of Biotechnology

IIT Hyderabad

Dr. Jyotsnendu Giri

Department of Biomedical Engineering

IIT Hyderabad

Acknowledgements

I would like to express my sincere gratitude to my thesis supervisor Dr. Basant Kumar Patel for his strong support in designing the experiment, troubleshooting the protocols and reviewing the project. I'm extremely thankful to him for the positive work space and moral support extended throughout the year.

I am deeply thankful for constructive criticism and review of my thesis committee members, Dr. Rajkumara Eerapa, Dr. Anamika Bhargava, Dr. Parag Pawar and Dr. Jyotsnendu Giri.

I extend my heartfelt thanks to my senior lab mates Vishwanath, Archana, Neetu Sharma, Amandeep Girdhar for providing a collaborative environment and timely help in completion of project.

I thank IIT Hyderabad for financial assistance in carrying out the project.

I am extremely grateful for my family for their endless support.

Abstract

Mutations in adenine biosynthesis pathway gene *ADE1* have been conventionally used to score for prion $[PSI^+]$ in yeast. If *ade1-14* mutant allele is present, which contains a premature stop codon, [*psi*] yeast appear red on YPD medium due to accumulation of a red intermediate compound in the vacuoles. In $[PSI^+]$ yeast, partial inactivation of the translation termination factor, Sup35 protein, due to its amyloid aggregation allows for read-through of the stop codon in the *ade1-14* allele and yeast appears white as no red intermediate pigment is accumulated. It is known that the red color development in *ade1* mutant yeast requires cytoplasmic levels of reduced glutathione which helps in transport of the intermediate metabolite P-ribosylaminoimidazole carboxylate (CAIR) into vacuoles that develops red color. Here, we hypothesized that amyloid-induced oxidative stress in yeast would deplete reduced glutathione levels and thus thwart the development of red color in the *ade1* yeast. Indeed, when we over-expressed amyloid forming human proteins TDP-43, Amyloid β-42 & Poly-Gln-103, the otherwise red *ade1* mutant yeast, turned to white color. Further, the color reverted back to red upon turning off the amyloid expression or by growth on media containing reducing agent thereby corroborating that the oxidative stress caused the white color. This red/white assay could also be emulated in an *ade1* yeast having *erg6* gene deletion that increases the cell wall permeability. Thus, this model would be useful tool for drug-screening against general amyloid-induced oxidative stress & toxicity in yeast.

KEYWORDS

Amyloid, TDP-43, Aβ-42, Oxidative stress, Adenine biosynthesis, Yeast prion $[PSI^+]$

Nomenclature

Genetic nomenclature

Gene symbol	Definition
ade1-14	Specific allele or mutation in ADE gene (Adenine)
his3-200	Specific allele or mutation in HIS gene (Histidine)
ura3-52	Specific allele or mutation in URA gene (Uracil)
leu2-3,112	Specific allele or mutation in LEU gene (Leucine)
trp1-289	Specific allele or mutation in TRP gene (Tryptophan)
erg6:TRP1	Insertion of functional TRP1 gene at ERG6 locus and erg6 is non-functional
[psi⁻]	Decreased efficiency of certain suppression (translational read through of stop codons in ade1-14 allele)
[PSI⁺]	Increased efficiency of certain suppression (translational read through of stop codons in ade1-14 allele)

Contents

Chapter 1

Introduction

1.1   Protein misfolding

Protein folding machinery ensures that the protein is packed into unique, three-dimensional native conformation to confer its functional activity. Protein folding is driven to attain maximum entropy and global energy minimum[1]. This self-organization of protein into native structure follows through the route of folding funnel[2]. Unique protein sequence drives the proteins from state of highest energy where the protein is unfolded to obtain lower energy states by local conformational arrangement to reach the unique native structure of protein with high entropy **(Figure 1)**[2].

The process is sophisticated and complex owing to the elaborate conventions of pathways involved and varying compartments in which it takes place. Inherent mutations and environmental agents such as temperature, pH, oxidation state contribute to the disruption of protein's native state resulting in protein unfolding[3]. The unfolded proteins, which are energetically unfavorable, seek to attain lower energy state causing protein misfolding and aggregation. The unfolded proteins can exhibit varying structural conformation from oligomers to amorphous aggregates to highly organized fibrils. Initially, misfolded proteins undergo intermolecular contacts to get organized into oligomers and form a nucleation core which binds misfolded

monomers reversibly. When a certain threshold critical mass is crossed, they form an irreversible large aggregate state with conformational plasticity (**Figure 1**). Low concentration of proteins tends to favor monomeric state whereas high concentration of proteins favor aggregation state.
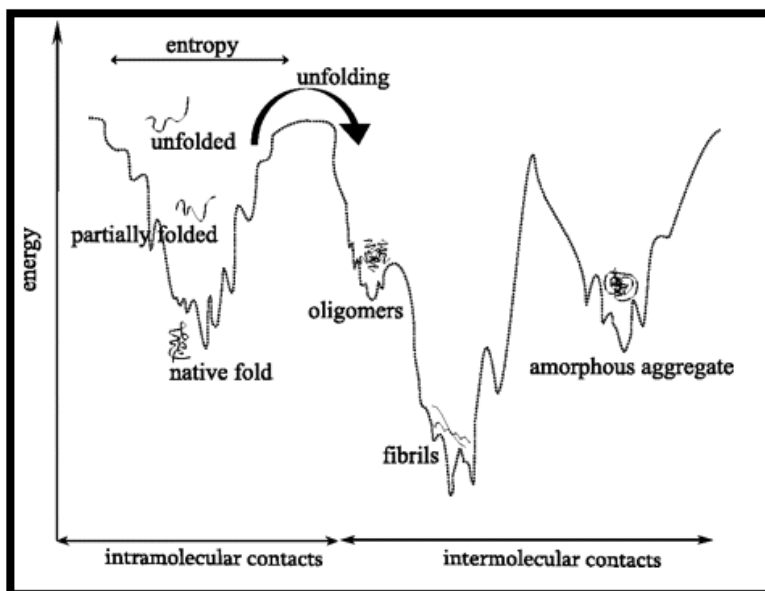

Figure 1: Energy state of protein folding and misfolding[2]

1.2   Amyloids and prions

Amyloid fibrils are stable, highly organized protein aggregates rich in β sheet conformation which forms abnormal, insoluble deposits in organs and tissues[4]. Conversion of peptide into fibrillar arrangement begins with a lag phase of forming nuclei followed by formation of series of metastable, non-fibrillar intermediates such as protofibrils. The fibrillar structure of amyloids consist of protofilaments 2-5 nm in diameter which can twist to form fibrils which are 7-13 nm wide[5] (**Figure 2A**). These large fibrils accumulate as proteinaceous deposits in amyloid and amyloid-like diseases (**Figure 2B**) [6]. Protofilaments are repeating units of "cross β" structure where β sheets are arranged parallel to fibrillar axis and its strands perpendicular to the axis. They are organized with an interstrand distance of 4.7 A° and intersheet space

distance of 10 A° [6, 7] (Figure 2C). Amyloids are characterized by the apple green birefringence with cross polarized light, upon binding to Congo red dye (Figure 2D) and increase in fluorescence upon binding to ThioflavinT (Figure 2E) [6]. Amyloids form detergent insoluble aggregates (Figure 2F) [8] which show partial resistance to proteinase K. Hydrophobic amino acids, β sheet predisposition and low net charge can enhance the formation of amyloids.
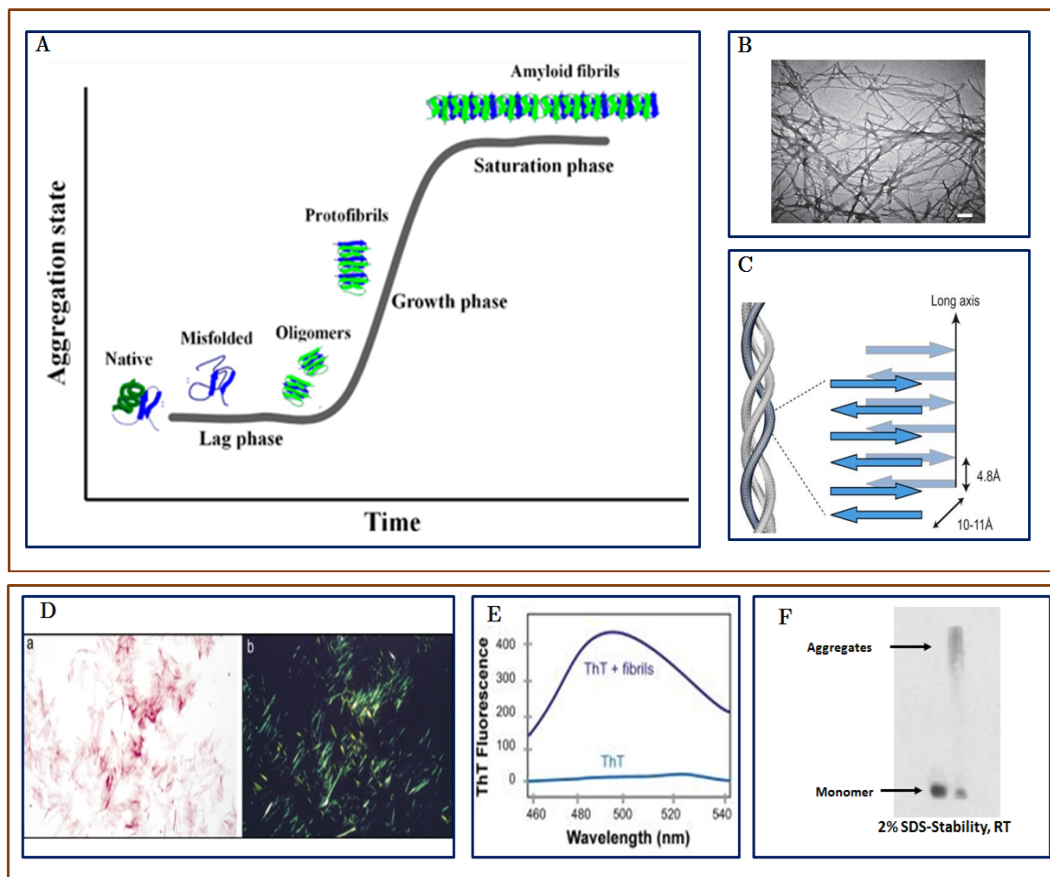

Figure 2: Amyloid fibrils and characteristics [5-8].

Amyloid deposits are reported in several neurodegenerative diseases including Alzheimer's and Parkinson's [3] (Table 1.1). Amyloids cause toxicity via number of pathways affecting Endoplasmic reticulum (ER) stress, Reactive Oxygen Species (ROS) and causing pores in lipid bilayers.

Table 1.1: Neurodegenerative diseases and associated proteins

Neurodegenerative disease	Associated proteins
Alzheimer's Disease	Aβ(40-42)
Frontotemporal dementia	Tau
Parkinson's Disease	α-Synuclein
Amyotrophic Lateral Sclerosis	TDP-43
Huntington's Disease	Huntingtin with PolyQ Expansion

Prions are infectious, self-propagating, transmissible protein isoforms that can fold in structurally distinct ways and cause diseases [9]. Prions are capable of transmitting their misfolded protein into a healthy species causing the properly folded protein structure to misfold and aggregate. Prions are reported in several organisms [10](**Table 1.2**).

Table 1.2: Prion diseases and host

Prion disease	Host
Familial Cruetzfeld Jacob Disease (CJD)	Human
Scrapie	Sheep
Bovine spongiform encephalopathy (BSE)	Cattle
Transmissible mink encephalopathy (TME)	Mink
Kuru	Fore people (Guinea)

1.3   Yeast as model of neurodegenerative diseases

Although yeast cell lacks specialized neuronal apparatus, yeast models have been extensively used for neurodegenerative diseases and have provided insights in the assembly of amyloid fibrils and their toxicity [11]. Being a eukaryote, yeast has several

conserved pathways such as cell division, transcriptional regulation, protein targeting and cytoskeletal dynamics, similar to mammals [12, 13]. Several prions have been identified in yeast (**Table 1.3**). The extensive understanding of molecular mechanisms of yeast prion aggregation has further helped in using yeast as a model for human amyloid diseases [9, 13-16]. As heterologous amyloid protein expression in yeast can lead to amyloid aggregation, large scale genetic and small molecule screens have been attempted for anti-aggregation or anti-toxicity of amyloid proteins from Alzheimer's, Huntington's and Amyotrophic lateral sclerosis diseases [17-19].

Table 1.3: Prions in yeast

Protein	Function	Prion form
Sup35	Translation termination	[PSI+]
Ure2	Nitrogen catabolite repression	[URE3]
Rnq1	Unknown	[PIN+]
Swi1	Chromatin remodeling	[SWI+]

Yeast prions have been extensively studied for red-white color phenotype. Conventionally, the *ade1* mutation has been used to score for yeast prion $[PSI^{+}]$ [16, 20]. If *ade1-14* allele is present, which contains a premature stop codon, $[psi]$ yeast appear red on YPD medium due to accumulation of a red intermediate compound in the vacuoles. In $[PSI^{+}]$ yeast, partial inactivation of the translation termination factor, Sup35 protein, due to sequestration into prion aggregates occurs. This allows for read-through of the stop codon in *ade1-14* allele, consequently no red intermediate pigment accumulates, thus $[PSI^{+}]$ yeast appear white color on YPD (**Figure 3**) [9]. $[PSI^{+}]$ yeast can grow on minimal media without adenine and Sup35-tagged GFP forms oligomer aggregates whereas $[psi]$ yeast cannot grow on minimal media without adenine and Sup35-tagged GFP remains diffused [9]. Likewise, a similar color assay for [URE3] prion in $[PSI^{+}]$ genetic background has also been developed using *ade1* mutation [21].
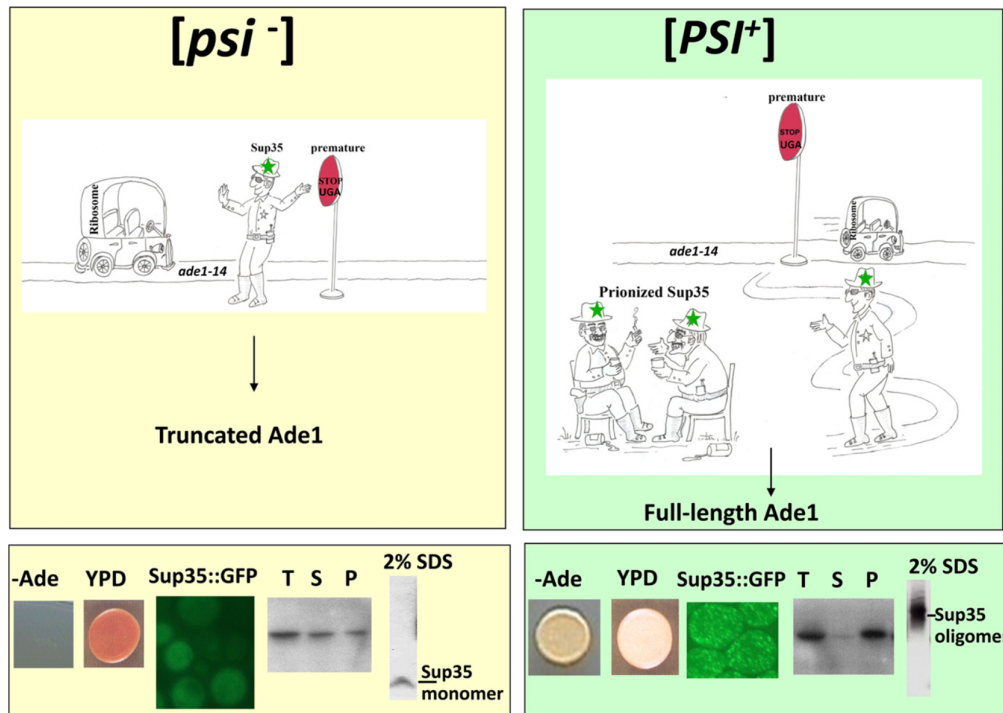
Figure 3: $[PSI^+]$ phenotypes [9]

1.4 Alzheimer's disease

Alzheimer's disease (AD) is a common neurodegenerative disorder resulting in progressive loss of memory and cognitive functions. Accounting for 60-80% of dementia, onset of Alzheimer's commonly begins after 65 years of age[22]. Genetic factors contribute in largest to the risk of AD while factors such as head injury, hypertension and depression are speculated to play a role in disease onset. Common symptoms of AD involve memory loss, disorientation, mood swings, behavioral problems and difficulties in language. AD causes large loss in weight and volume of the brain in turn reflecting as loss of neuronal processes. AD brain is characterized by the accumulation of extracellular amyloid plaques and intracellular neurofibrillary tangles composed of aggregated Amyloid β (Aβ) and Tau proteins respectively [23] (**Figure 4A**). With 48 million people reported to suffer from AD, as of 2015, the need for understanding and combating toxicity mechanisms has become more relevant.
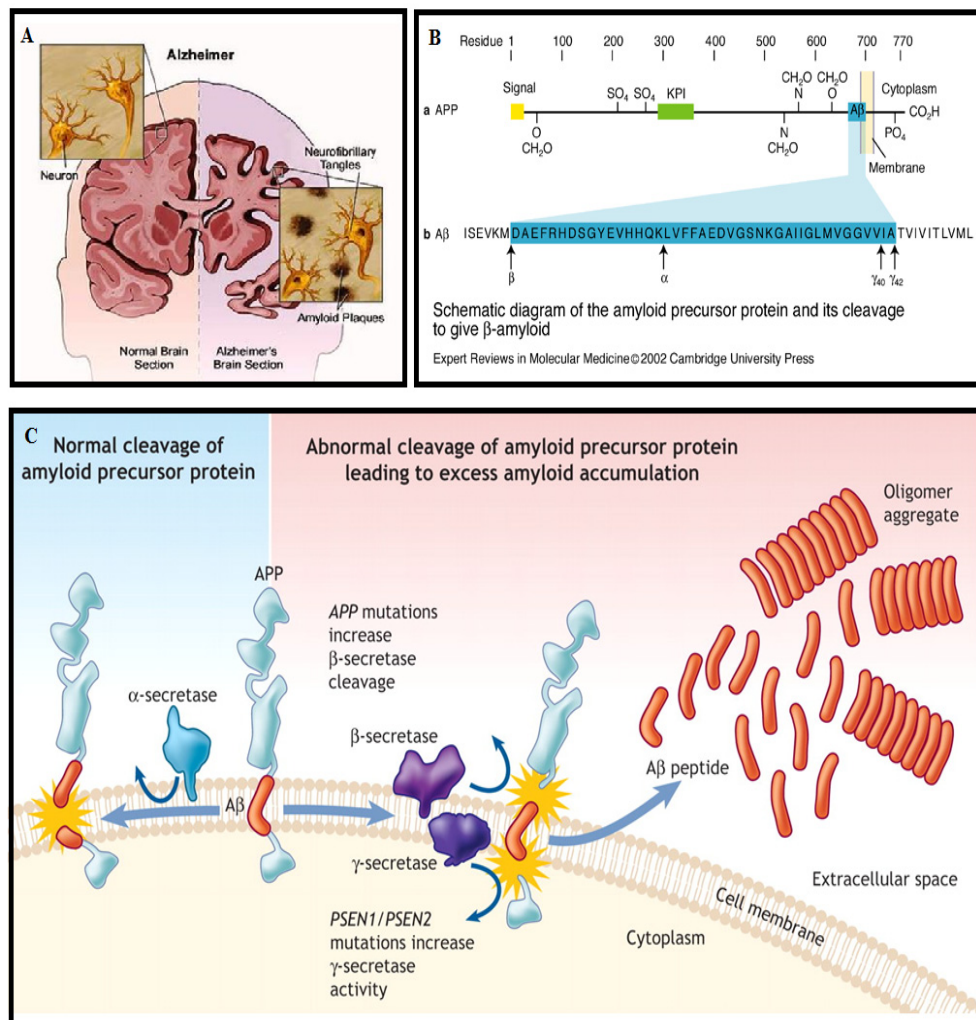
Figure 4: Alzheimer's pathology and APP processing [23]

In Alzheimer's pathology, amyloid beta-42 (Aβ-42) peptide produced from Amyloid Precursor Protein forms amyloid plaques and is implicated in progression of disease [24]. Amyloid precursor protein (APP) is a single pass transmembrane protein with eight isoforms, of which 695 amino acid (aa) is predominant in CNS and 751 aa, 770 aa are ubiquitous [25]. APP processing plays a crucial role in the AD pathology. Three different secretases, α secretase, β secretase and γ secretase vary in the key residues they cleave (Image: Qi Chen and David Schubert, Expert reviews in Molecular Medicine 2002) **(Figure 4B)**. In cell surface, APP is normally cleaved by α

secretase in which case Aβ-42 residues are not formed. However, when APP is cleaved by β and γ secretase, variable Aβ polypeptide containing 37-49 residues are formed [23] **(Figure 4C)**.

Accumulation of Aβ in brain is shown to cause aberrant stimulation of Glutamate receptors causing excitotoxicity and synaptic depression [26]. Epileptic seizures [27] and reduction in Voltage Gated Sodium Channels (VGSC) are also evident in patients suffering from AD [28]. Current drug targets for AD include acetylcholine esterase whose inhibition can elevate depleted acetylcholine levels in human brain [29], β and γ secretase [30, 31] whose inhibition can possibly inhibit Aβ precursor formation, modulation of Tau phosphorylation [32, 33] and regulation of apoE4 levels[34].

When Aβ-42 was expressed in yeast, it was found to form detergent stable oligomers suggesting amyloid-like structure and this model has been used for drug screening [18, 35]. In the yeast model, when Aβ-42 peptide is directed towards the secretory pathway it was found to increase oxidative stress and mitochondrial dysfunction [36].

1.5   Huntington's disease

Huntington's disease (HD) is a neurodegenerative disorder which predominantly affects muscle coordination, personality changes and behavior. HD is an autosomal dominant disorder which becomes clinically symptomatic at 35-40 years. Expansion of CAG repeats in the gene coding for Huntingtin (HTT) protein encodes an abnormal protein which has tendency to aggregate. In Huntington's disease, mutant extension of Poly-Gln(Q) stretches beyond 39 glutamine encoded by *huntingtin* exon1, have been linked to amyloid aggregation and pathogenesis [37].

Full length HTT protein as well as an amino-terminal HTT exon fragments formed undergo proteolysis to generate fragments which can aggregate in nucleus, where it causes transcriptional dysregulation and in cytoplasm where it causes mitochondrial toxicity, synaptic dysfunction and axonal transport impairment **(Figure 5)** [37].

8
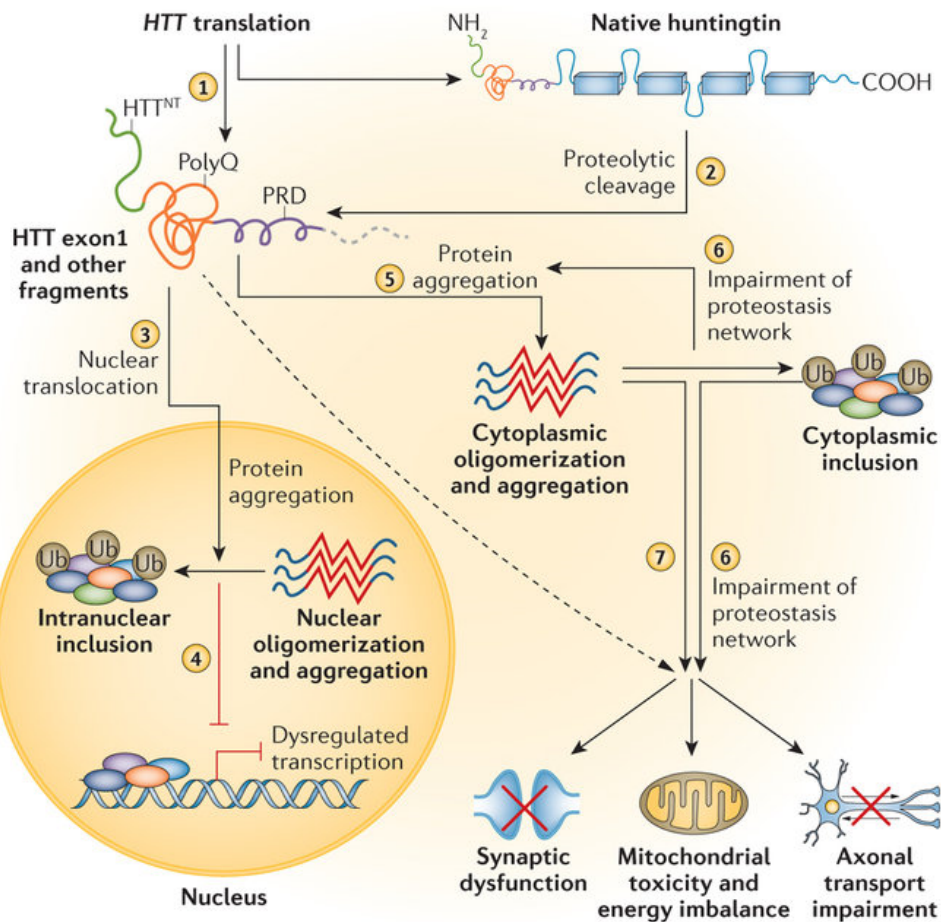
Figure 5: Pathogenic cellular mechanism of Huntington's disease[37].

Gene silencing, recovery of mitochondrial function, HTT lowering and immunomodulation has been tried as therapeutic strategies for HD. Current drugs in clinical trials aim to alleviate the symptoms of motor system dysfunction. TetraBenaziene and Cysteamide bitarttrate delayed release capsule are in clinical trials which aim to restore muscle coordination [37].

A simulative aggregation of Poly-Q-GFP in yeast model also occurs if the number of Gln residues are more than 40 and this aggregation is also associated with toxicity [38]. Presence of prion-like protein Rnq1 is indispensable for PolyQ toxicity in yeast [38, 39]. Further, acceleration of Sup35 fiber formation by heterologous aggregate

forming proteins of PolyQ established a link between the prions and Huntington's[40]. Huntingtin Poly-Q aggregation can also alter mitochondrial morphology and compromise mitochondrial function, with early alterations in complexes II and III of the respiratory chain leading to an increase in ROS production [12, 41]. Yeast models of PolyQ tracts have also been widely used as high throughput screen for small molecules [42-44] that enhances autophagy and reduce toxicity [45].

1.6 Amyotrophic lateral sclerosis

Amyotrophic lateral sclerosis (ALS) is a fatal neurodegenerative disorder which affects the motor neurons, resulting in muscular atrophy, muscle twitching, progressive weakness and death within few years. 90% of ALS cases are sporadic whereas 10% can be attributed to familial mutations. Trans active response (TAR) DNA binding protein (TDP) is a 43 kDa nuclear protein encoded in chromosome 1. TDP-43 is a highly conserved protein which contains two RNA recognition motifs (RRM 1&2) and a glycine rich C-Terminal region [46] **(Figure 6)**. It is speculated to play an important role in transcriptional repression and pre-mRNA splicing.
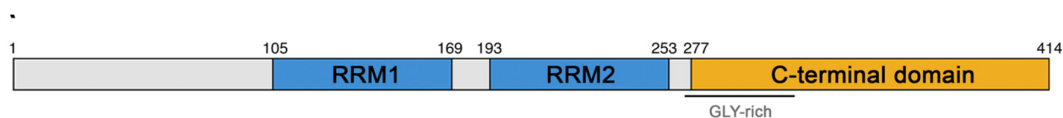
Figure 6: Domain architecture of TDP-43 [46]

Soluble TDP-43 is ubiquitously present in the nucleus can mislocalise to cytoplasm and form toxic inclusions depleting the nuclear pool of TDP-43. Pathological TDP-43 is hyper phosphorylated, ubiquitinated and cleaved to produce C terminal fragments which are capable of aggregating in cytoplasm [47] **(Figure 7).** Aggregation of TAR DNA-binding protein-43 (TDP-43) either of wild-type or familial mutant protein sequence into detergent stable structures suggests the presence of amyloid nature [48-50].

Figure 7: TDP-43 aggregation [47]

Therapeutic targets of ALS have been to prevent cytoplasmic mislocalisation[51, 52], ubiquitination of TDP-43 [53], fragmentation and ag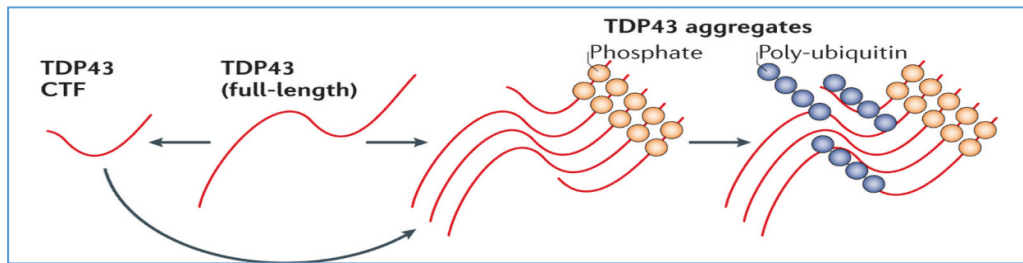gregation of TDP-43 [54] and environmental stress [48]. Owing to the complexities of pathways involved, therapeutic approaches in clearing TDP-43 and mitigating ALS has not been successful. However, there are few drugs which is given to reduce the symptoms, especially motor system dysfunction and improve quality of life after ALS. Riluzole is an FDA approved drug to reduce damage to motor neurons.

Strikingly, TDP-43 can also aggregate in the yeast model and shows toxicity. Also it shares requirement of several factors such as ataxin-2 homolog, PBP1, modulating its aggregation and toxicity thereby suggesting a validity of this yeast model to the human ALS [17]. Two ALS mutants R524S or P525L has been reported to show increased toxicity in yeast [55]. In yeast, expression of TDP-43 can trigger oxidative stress & apoptosis and mitochondrial respiration was found to be an important modulator of the cytotoxicity [56]. Unbiased yeast genetic screens have been used to identify suppressors of TDP43 toxicity [17].

1.7   Hypothesis: Amyloid-induced oxidative stress in yeast

The host yeast cell used for the over-expression of amyloid proteins Aβ-42-EGFP, Poly-Q$_{103}$-GFP or TDP-43-YFP contained *ade1-14* mutant allele which contains a premature stop codon in *ADE1* gene and is consequently defective in adenine biosynthesis that causes red-color phenotype on YPD-agar media due to accumulation of a red intermediate metabolite in the vacuoles of these cells [9, 57]. It is known that the development of red color in *ade1* mutant yeast requires cytoplasmic levels of

reduced glutathione which helps in transport of the intermediate metabolite P-ribosylaminoimidazole carboxylate (CAIR) into vacuoles and the subsequent development of color [57, 58]. Here, we hypothesized and examined if amyloid-induced oxidative stress in yeast would deplete reduced glutathione levels and thus thwart the development of the red color in the *ade1* mutant background upon overexpression of Aβ-42-EGFP, Poly-Q$_{103}$-GFP or TDP-43-YFP amyloid proteins **(Figure 8)**
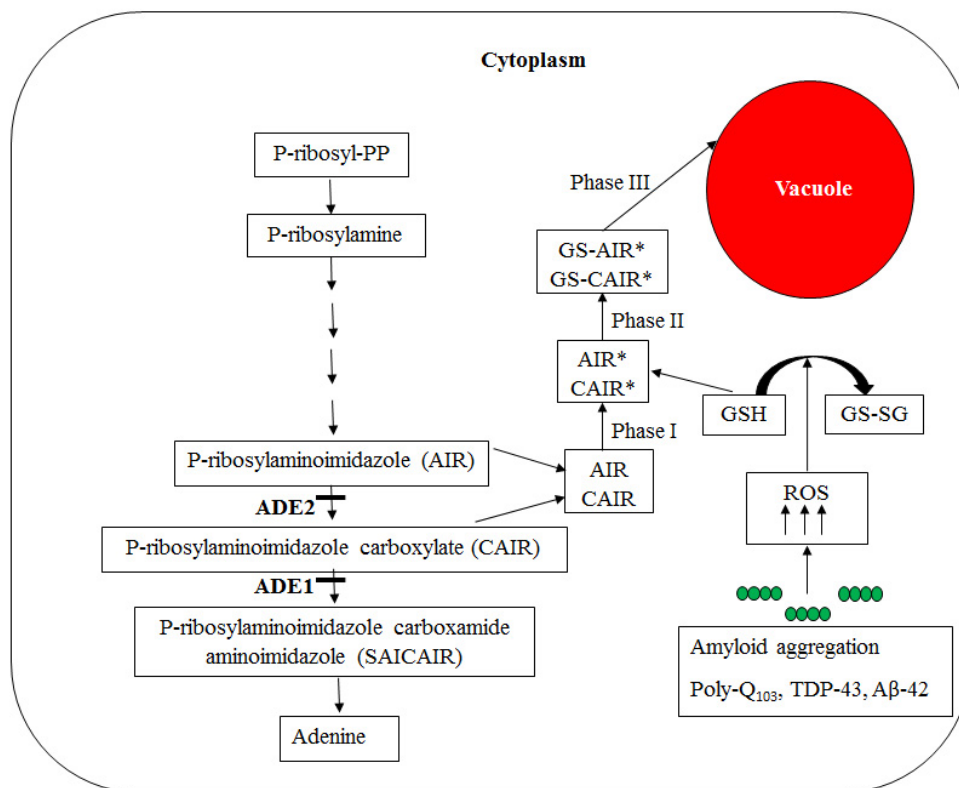
Figure 8: Hypothesis pathway for amyloid-induced oxidative stress in yeast.

Chapter 2

Materials and Methods

2.1 Materials

2, 3, 5-Triphenyl Tetrazolium Chloride, L-ascorbic acid, D-raffinose, D-galactose, Ampicillin and Lithium acetate were purchased from Sigma (USA). D-Glucose was procured from Amresco (USA). Yeast nitrogen base, yeast extract, peptone, DMSO, agar and glass slides were procured from HiMedia (India). Salmon sperm DNA was purchased from Invitrogen (USA).

2.2 Yeast strain and plasmid

The [*psi*] [*pin*] and [*psi*] [*PIN⁺*] yeast strains were derivatives of 74-D-694 (*MATa ade1-14 his3-200 ura3-52 leu2-3, 112 trp1-289*)[59]. Assays were performed in [*psi*] [*pin*] strain containing pRS416 [60] or pRS416-GAL1p-Aβ-42-EGFP (URA3) (A kind gift of Prof. Susan Liebman, University of Nevada, Reno, USA) or pRS416-GAL1p-TDP43-YFP (URA3) (Addgene: 27447) and in a [psi⁻] [PIN⁺] strain containing pRS416-GAL1p-Q$_{103}$-GFP (URA3) (Addgene: 1186). Yeast strain L-3341, *MATα ade1-14 leu2-3,112 trp1-289 ura3-52 lys9-A21 erg6::TRP1* [*PIN⁺*] [18], a derivative of 64-D, was a kind gift of Prof. Susan Liebman, University of Nevada, Reno, USA.

2.3 Bacterial culture media

Luria Bertani (LB) + Ampicillin media was used for reviving and maintaining the bacterial transformants containing pRS416 [60], pRS416-GAL1p-Aβ-42-EGFP

(URA3), pRS416-GAL1p-TDP43-YFP (URA3), pRS416-GAL1p-Q$_{103}$-GFP (URA3) plasmids. These plasmids have ampicillin as antibiotic selection marker. LB media contains Tryptone (1%), yeast extract (0.5%) and sodium chloride (1%). pH was adjusted to 7 using sodium hydroxide and for preparation of solid media 1.5% agar was used. Media was autoclaved foe 20 minutes at 121 ˚C. Media was cooled and 50 µg/mL ampicillin was added to media.

2.4   Yeast culture media

Standard yeast media and cultivation conditions were used [61]. Yeast cells were grown in complex media (YPD) or in a standard synthetic medium lacking a particular amino acid and containing either D-glucose (SD) or L-raffinose (SRaf) as the sole carbon source. Galactose (2%) was used to over-express GAL1 promoter driven genes. Red-white color switch was scored on SRaf-agar lacking Uracil (Ura), but containing one-fourth amount of yeast extract and peptone compared to YPD and 0.1% galactose (SRaf-agar-Ura+0.1% Gal+$\frac{1}{4}$ YP). Complete loss of mitochondrial was scored by lack of growth on complex media containing 2% glycerol as the only carbon source (YPG-agar). Effect of ascorbic acid (AA) on red-white color switch was scored in SD-agar lacking Uracil (Ura), and containing 10 mM ascorbic acid and also added with $\frac{1}{4}$ YP (SD-agar-Ura+$\frac{1}{4}$ YP+10 mM AA).

2.5   Plasmid isolation

Plasmids pRS416, pRS416-GAL1p-Aβ-42-EGFP (URA3), pRS416-GAL1p-TDP43 YFP (URA3), pRS416-GAL1p-Q$_{103}$-GFP (URA3) are low copy number yeast centromeric plasmids (YCP) under Gal1 promoter.

Mini Prep

Plasmids were isolated using GeneJet Thermoscientific kit.

1. Bacterial transformants were grown in LB-amp broth in rotary shaker at 200 rpm for 12-16 hours at 37 ˚C.

2. Cells were pelleted by centrifuging at 8000 rpm for 2 minutes and the supernatant was decanted.

3. Cells were resuspended in 250 µL of resuspension solution. Cell suspension was transferred to microcentrifuge tube.

4. 250 µL of lysis solution was added and mixed thoroughly by inverting the tube 4-6 times until the solution becomes viscous and slightly clear.

5. 350 µL of neutralization solution was added and mixed immediately and thoroughly by inverting the tube 4-6 times and centrifuged at 10,000 rpm for 5 minutes to pellet cell debris and chromosomal DNA.

6. Supernatant was transferred to spin column by pipetting and centrifuged for 1 minute and flow through was discarded and column was placed back into same collection tube.

7. 500 µL of wash solution was added to column and centrifuged for 1 minute and flow through was discarded and step was repeated.

8. Column was transferred to 1.5 mL microcentrifuge tube and 50 µL of elution buffer was added to center of column to elute DNA and incubated for 2 minutes at room temperature and centrifuged for 2 minutes.

9. DNA was stored at -20 °C until further use.

2.6   Transformation of yeast

Transformation of yeast with plasmids was carried out using the standard Li-Acetate method [61].

1. Single yeast colony was inoculated in 5 mL YPD and grown overnight broth in rotary shaker at 200 rpm at 37 °C.

2. 0.5 mL of culture was added to 4.5 mL fresh media and grown till it OD_{660nm} was approximately 1.0.

3. Cells were spun down at 3000g for 5 minutes and washed with 10 mL sterile water and centrifuged at 3000g for 5 minutes. Pellet was resuspended in 1 mL sterile water and transferred to 1.5 mL microcentrifuge tube, spun down and resuspended in 1 mL sterile TE/LiAc buffer.

4. 250 µL of yeast cells were transformed with 5 µL of plasmid, 5 µL of single stranded carrier DNA (10 mg/mL) [boiled and quick chilled on ice] in a 1.5 mL microfuge tube. 300 µL of sterile PEG was added and mixed thoroughly.

5. Tube was incubated at 30 °C for 60 minutes with occasional gentle shaking.

6. 40 µL of DMSO was added and mixed thoroughly.

7. Heat shock was given at 42 °C for 15 minutes and ice for 2 minutes and spun for 1 minute at 14000 rpm to remove supernatant, resuspended in1 mL 1X TE. Tube was spun again for 10 second and resuspended in 1 mL 1X TE. 200 µL was plated on selective media and the plate was incubated at 30 °C until colonies appear.

2.7   Fluorescence microscopy

For fluorescence microscopy, single colony isolates of yeast plasmid transformants were grown overnight at 30 °C in SRaf-Ura broth media. Then, the cells were re-suspended in fresh media and expressions of TDP-43-YFP, Poly-Q$_{103}$-GFP or Aβ-42-EGFP were induced with 2% galactose for 8-24h before harvesting the cells for microscopy. Fluorescence was observed under Leica DM-2500 microscope and images were acquired using 100x objective lens (oil immersion) in bright field or by using the GFP filter and processed using ImageJ software [62].

2.8   Petite colony assay

Single cell colony isolates were grown in selective media SRaf-Ura at 30 °C overnight and induced with 2% Gal to express the constructs. After appropriate time, appropriate dilutions were made and cells were plated on YPD to observe petite colony count. For TDP-43-YFP and PolyQ-103-GFP, the colonies were plated after 24 hours when aggregates are formed. For Aβ-42-EGFP the colonies were plated after 8 hours of galactose induction.

2.9   Red white colony assay

Single cell colony isolates were grown in selective media SRaf-Ura at 30 °C overnight and induced with 2% Gal to express the constructs. After appropriate time,

appropriate dilutions were made and cells were plated on SRaf-Ura+ $\frac{1}{4}$ YP+0.1% Gal to visualize red and white colonies. For TDP-43-YFP and PolyQ-103-GFP, the colonies were plated after 24 hours when aggregates are formed. For Aβ-42-EGFP the colonies were plated after 8 hours of galactose induction.

2.10   Triphenyl tetrazolium chloride (TTC) assay

2, 3, 5-triphenyltetrazolium chloride (TTC) was used as a color indicator for dehydrogenase enzymes. For this, molten soft agar (1.5%) containing 0.1% of TTC was gently poured onto yeast patched pre-grown on SRaf-agar-Ura+0.1% Gal. Plates were incubated at 30° C for 2 hours and then imaged [63-65].

2.11   Growth assay on ascorbic acid

Yeast cells when grown on media containing small reducing agents can take up the reducing agents leading to neutralization of the any cytoplasmic oxidative stress [66]. The yeast cells plated in SRaf-agar-Ura+0.1% Gal after the prior overexpression of amyloid protein (TDP-43-YFP) with 2% galactose were patched on SD-agar-Ura+ $\frac{1}{4}$ YP and SD-agar-Ura+ $\frac{1}{4}$ YP+10 mM AA. Cells were serially passaged by patching on the same media and examined for color in each passage.

17

Chapter 3

Results and discussion

3.1   Aggregation of amyloid proteins causes red to white color switch in *ade1* mutant yeast

Usually, when Sup35 protein, which is a translation termination factor, is over-expressed it leads to prion conversion to $[PSI^+]$ that partially inactivates Sup35 protein thereby allowing read-through of the premature stop codon in *ade1-14* allele. This leads to functional ADE1 protein formation that allows for growth on media lacking adenine and also, the red intermediate pigment does not accumulate hence the $[PSI^+]$ yeast is white on YPD-agar. Thus, this red to white conversion in *ade1-14* allele containing yeast strain (e.g. 74-D-694) upon over-expression of Sup35 protein is scored as *de novo* $[PSI^+]$ prion formation [14, 20]. Alternatively, if *ade1-14* yeast lose their mitochondria and become petite (i.e. [*rho*-]), they also exhibit red to white color phenotype switch on the YPD-agar media [59].

When TDP-43-YFP, Aβ-42-EGFP or Poly-Q$_{103}$-GFP were over-produced from a plasmid in a yeast cell using induction of their galactose-inducible promoter by addition of 2% galactose in the media, punctate fluorescent foci were formed for each of these proteins (**Figure 9**). This is as expected upon their amyloid-like aggregations in the cell which has also been previously established [38, 46, 67].
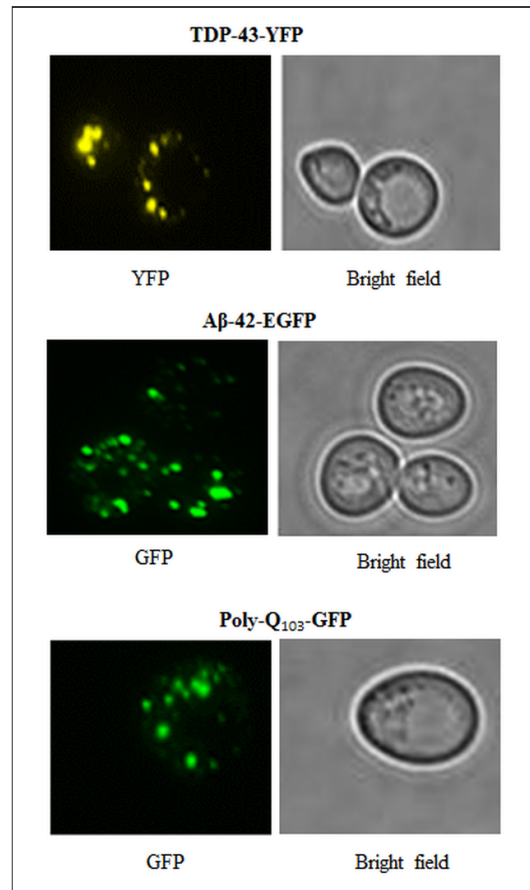
Figure 9: Aggregation of TDP-43-YFP, Aβ-42-EGFP or Poly-Q$_{103}$-GFP in yeast cell

When TDP-43-YFP, Aβ-42-EGFP and PolyQ-103-GFP amyloid forming proteins were already over-expressed by pre-growth in presence of 2% galactose for 24 h, 8 h and 24 h respectively and plated on YPD (**Figure 10**) to assess the petite cells (which has lost mitochondria), we found that only 0.1% of the TDP-43-YFP colonies, 1.3% of the Aβ-42-EGFP colonies, & 1.2% of the Poly-Q$_{103}$-GFP colonies, were found to be petites (indicated by black arrow).
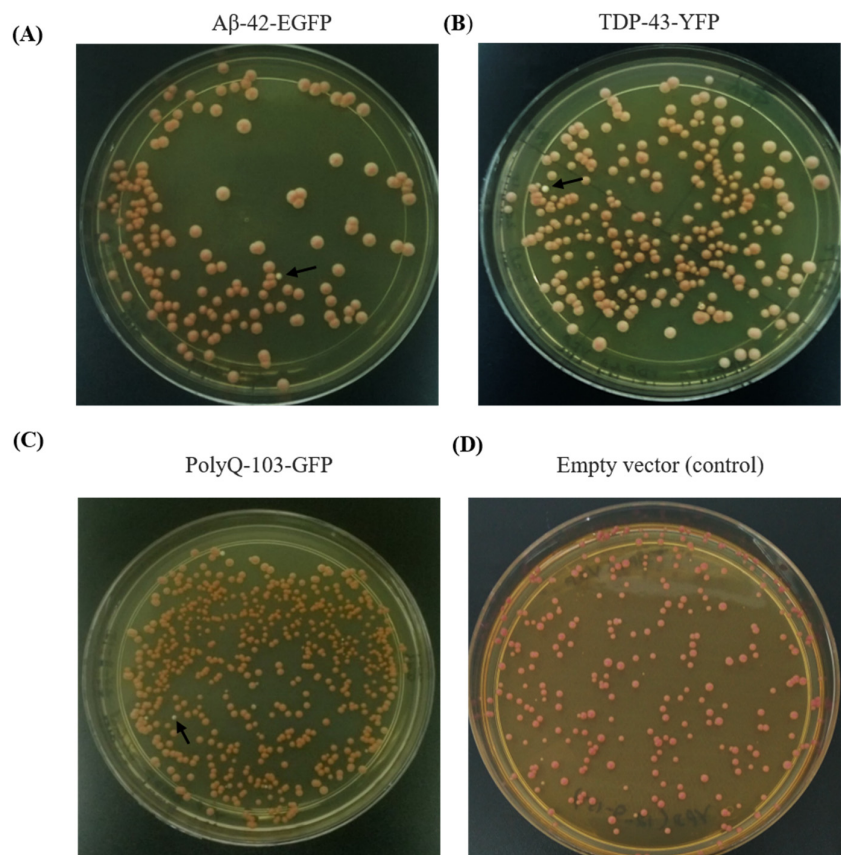
19

Figure 10: Petite assay on YPD after amyloid overexpression

Strikingly, when we plated the *ade1-14* allele bearing [*psi*] [*pin*] yeast cells onto SRaf-agar-Ura+0.1%Gal+ ¼ YP where TDP-43-YFP, Aβ-42-EGFP amyloid forming proteins were already over-expressed by pre-growth in presence of 2% galactose, ~100% (**Table 3.1**) of colonies from both appeared to have switched to white color (**Figure 11**). The addition of one-fourth yeast extract and peptone (i.e. ¼ YP) compared to YPD-agar, allows for red color development in an *ade1-14* allele bearing yeast cell while also maintaining the plasmid selection. Furthermore, when Poly-Q_{103}-GFP was over-expressed using 2% galactose in *ade1-14* allele bearing [*psi*] [PIN^+] yeast, ~10.9 % (**Table 3.1**) of colonies for Poly-Q_{103}-GFP appeared white color on SRaf-agar-Ura+0.1%Gal+¼ YP plates.
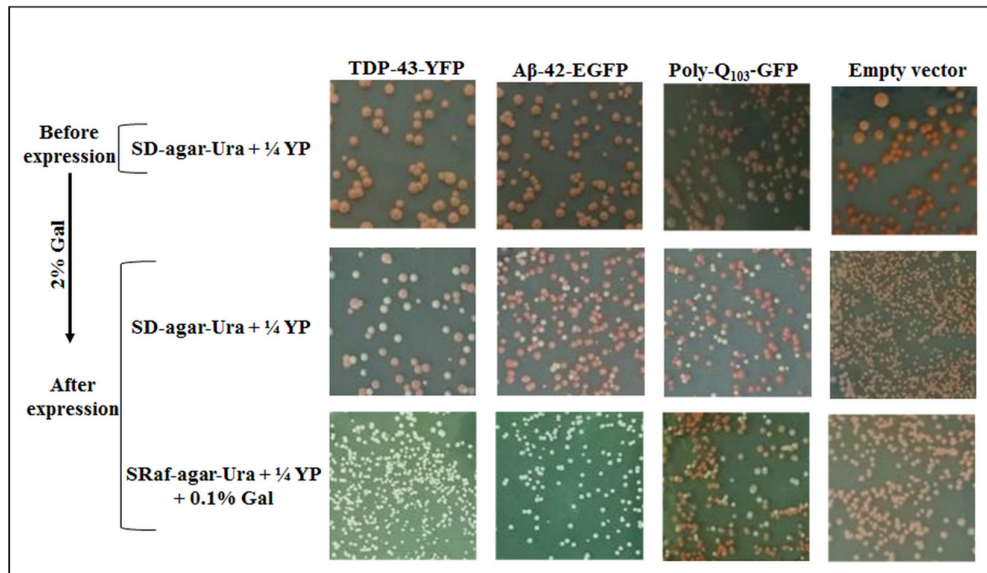
Figure 11: Amyloid protein expression causing red to white color switch in ade1-14 mutant yeast

Table 3.1: Red white colony assay in TDP-43-YFP, Aβ-42-EGFP, PolyQ-103-GFP On SRaf-Ura+ $\frac{1}{4}$ YP+ 0.1% Gal

Amyloid Proteins	Total colonies	Red colonies	White colonies	Pink colonies	Percentage of white colonies
TDP-43-YFP	1050	0	1050	0	100
PolyQ-103-GFP	1009	899	110	0	10.9
Aβ-42-EGFP	289	0	289	0	100

When we examined these white color colonies obtained after over-expressions of the TDP-43-YFP, Aβ-42-EGFP or Poly-Q$_{103}$-GFP proteins, for growth on medium lacking adenine (SD-agar-ade), the failed to grow. This is as expected, in the view that the growth on SD-agar-ade would require that the cells are $[PSI^+]$, which in turn requires

21

prior Sup35 over-production [9, 14]. Additionally, when we checked if these white colonies were formed by petite cells, by assessing growth on media containing glycerol as the only carbon source (YPG-agar) that allows growth of only cells bearing functional mitochondria, majority of the white colonies showed positive growth on YPG-agar (**Figure 12**).
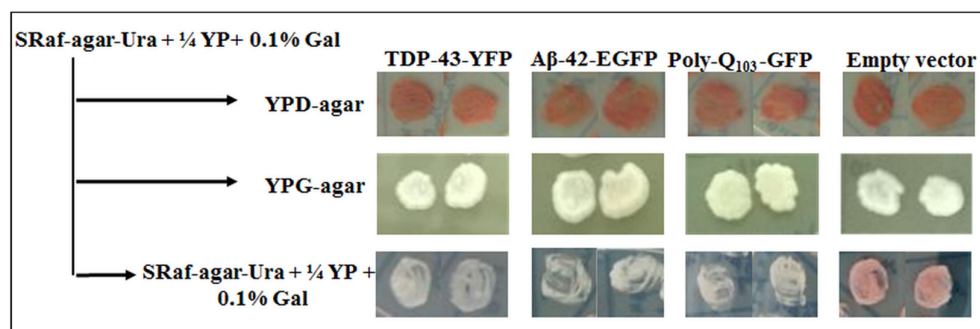

Figure 12: White color switch is not due to complete mitochondrial loss.

In the view that majority of the white colonies were neither [*PSI$^+$*] nor petites, we set forth to examine the mechanistic cause for the red to white color switch. For this, as the formation of the intermediate metabolite due to the pre-mature nonsense mutation in *ade1-14* allele is not expected to be hindered in a non-[*PSI$^+$*] cell, we reasoned that possibly the development of the red color from this intermediate (CAIR) is instead being interfered with, upon the over-expressions and cellular aggregations of these TDP-43-YFP, Aβ-42-EGFP or Poly-Q$_{103}$-GFP amyloid-forming proteins. It is previously known that the aggregation of these amyloid-like proteins can cause general cytotoxicity by several mechanisms such as impairing protein homeostasis, over-engaging cellular chaperones or by causing oxidative stress etc. [38, 46, 68]. Also, it has been previously demonstrated that reduced glutathione-mediated transport of the intermediate metabolite, CAIR, to the vacuoles in an *ade1* mutant yeast, is required for the development of the red color [57]. Thus, we hypothesized that possibly the accumulation of these amyloid aggregates leads to oxidative stress that could deplete the levels of reduced glutathione by oxidizing it. In turn, even after

being synthesized the intermediate metabolite in the *ade1* mutant yeast would not be transported to the vacuoles and thus the red color would not develop thereby imparting white color to the host yeast.

3.2   Red to white color switch is reversible

When the yeast cells SRaf-Ura+0.1% Gal were passaged on YPD, SD-Ura+1/4YP and SRaf-Ura+0.1% Gal+1/4 YP, after first passage white colonies from TDP-43-YFP, Poly-Q$_{103}$-GFP turned 100% red on YPD, 100% white on SRaf-Ura+0.1% Gal+1/4 YP whereas in SD-Ura+1/4 YP, white colonies turned pink. In Aβ-42-EGFP, after first passage on SD-Ura $+ \frac{1}{4}$ YP, 87.5% cells turned pink (**Table 3.2**).

If the white color switch was due to induction of oxidative stress by amyloid aggregation and not due to a suppressor genetic mutation(s) or reversion of the *ade1-14* allele to wild-type *ADE1* allele, the yeast would be expected to switch back to red color once the oxidizing environment is over. To check this, we examined if sequentially passaging these white colonies on SD-agar-Ura+$\frac{1}{4}$ YP, where the expressions of these amyloid forming proteins would be turned-off, leads to reversion to the red color phenotype. Indeed, we observed that after three passages on SD-agar-Ura+$\frac{1}{4}$ YP, the white cells returned back to the red color phenotype (**Figure 13**).

Table 3.2: Red white colony count after first passage on different media

| Amyloids	Media	Red	White	Pink	Percentage
TDP-43-YFP White (22 colonies)	YPD	22	0	0	100% Red
	SD-Ura + $\frac{1}{4}$ YP	0	16	6	27% Pink, 72.7% white
	SRaf-Ura + $\frac{1}{4}$ YP +0.1% Gal	0	22	0	100% white
PolyQ-103-GFP Red (16 colonies)	YPD	16	0	0	100% Red
	SD-Ura + $\frac{1}{4}$ YP	16	0	0	100% Red
	SRaf-Ura + $\frac{1}{4}$ YP +0.1% Gal	0	0	16	100% Pink
PolyQ-103-GFP White (15 colonies)	YPD	15	0	0	100% Red
	SD-Ura + $\frac{1}{4}$ YP	0	15	0	100% white
	SRaf-Ura + $\frac{1}{4}$ YP +0.1% Gal	0	15	0	100% white
Aβ-42-EGFP White (16 colonies)	YPD	16	0	0	100% Red
	SD-Ura + $\frac{1}{4}$ YP	16	0	0	100% Red
	SRaf-Ura + $\frac{1}{4}$ YP +0.1% Gal	0	2	14	87.5% Pink, 12.5% white
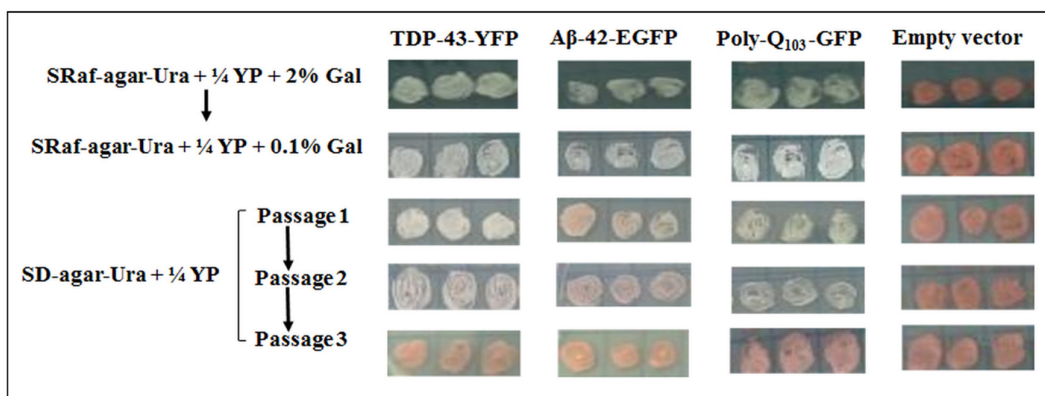
Figure 13: White color switch is reversible

In contrast, when the white cells were passaged similarly on media that allowed for even milder continued expression of these amyloid proteins using 0.1% galactose (on SRaf-agar-Ura + 0.1% Gal+$\frac{1}{4}$YP), the cells retained their acquired white color phenotype (**Figure 12**). Additionally, the acquired white phenotype rapidly converted to red color even upon the first passage on the complex complete media YPD-agar possibly due to its greater buffering ability against oxidative stress (**Figure 12**).

3.3   White yeast colonies exhibit signs of oxidative stress

While the above data are consistent with presence of oxidizing environment in white colonies obtained after over-expressions of the TDP-43-YFP, Aβ-42-GFP or Poly-Q$_{103}$-GFP amyloid-forming proteins, we further attempted to experimentally establish the presence of oxidative stress in these cells. It is known that oxidative stress can damage mitochondria thereby leading to its leakiness & causing enhanced release & secretion of mitochondrial redox enzymes such as dehydrogenases [65].Therefore, we assayed the relative levels of available dehydrogenases by reaction with a probe organic substrate 2,3,5-triphenyl tetrazolium chloride which develops red color after being acted upon by dehydrogenase enzymes [63-65, 69]. Indeed, when tested directly on patches of yeast cells over-expressing either the TDP-43-YFP or a control empty vector, the amyloid-expressing cells developed red color relatively faster and also with

higher intensity (**Figure 14**). This data confirms elevated presence of dehydrogenases and are suggestive of presence of mitochondrial damage.
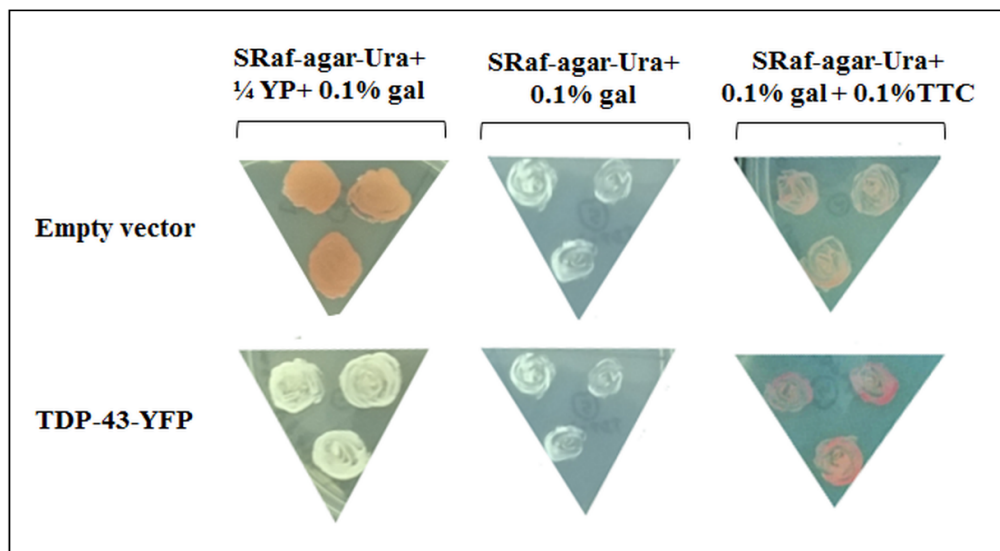

Figure 14: TTC method for assessment of presence of mitochondrial damage

Furthermore, if the white yeast cells have oxidizing cellular environment, growth on media containing a reducing agent, such as ascorbic acid, would be expected to restore the red phenotype back. Reducing agent could prevent the oxidation of the reduced glutathione and allow for the transport of the adenine biosynthesis intermediate metabolite to the vacuoles thereby helping in red color development. Indeed, when we plated the white cells on medium containing 10 mM ascorbic acid, the color transitioned to red thereby corroborating our assumption of presence of oxidizing stress in the amyloid-expressing cells (**Figure 15**). In controls, when we likewise plated [*PSI*$^+$] cells on this ascorbic acid medium, the cells continued to retain their white color phenotype.
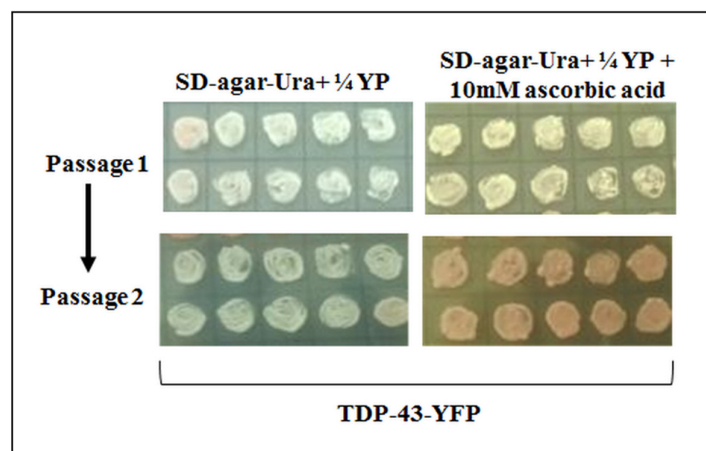
Figure 15: Growth on ascorbic assay to assess oxidative stress

This is consistent with the expectations as the $[PSI^+]$ cells do not produce the adenine biosynthesis intermediate metabolite and therefore cannot develop the red color even if the cytoplasm becomes more reducing in nature thereby the elevating reduced glutathione cytoplasmic levels. Notably, in presence of ascorbic acid, the overall intensity of the red color was relatively less, possibly due to other pleiotropic effects of ascorbic acid on the yeast physiology.

3.4   Amyloid-induced red to white switch also occurs in *erg6Δ ade1-14* double mutant yeast

Yeast models of amyloid aggregation have been previously utilized to screen for drug-like anti-aggregation molecules such as against Aβ-42 aggregation [18]. The designed red-white assay here would be easily applicable for such screening of anti-amyloid small molecules due to its simplicity. As yeast cell wall is generally impervious to small drug-like molecules, we examined if the red-white color assay can also be recapitulated in an *erg6Δ* yeast which, due to defective ergosterol biosynthesis, increases the permeability of the yeast cell wall [57, 70, 71]. For this, we transformed an *erg6Δ* derivative yeast of 64-D strain, which also contains the *ade1-14* mutant allele, with the galactose inducible TDP-43-YFP expression plasmid. Alike in the 74-D694 yeast strain containing the *ade1-14* allele, over-expression of TDP-43-YFP in

27

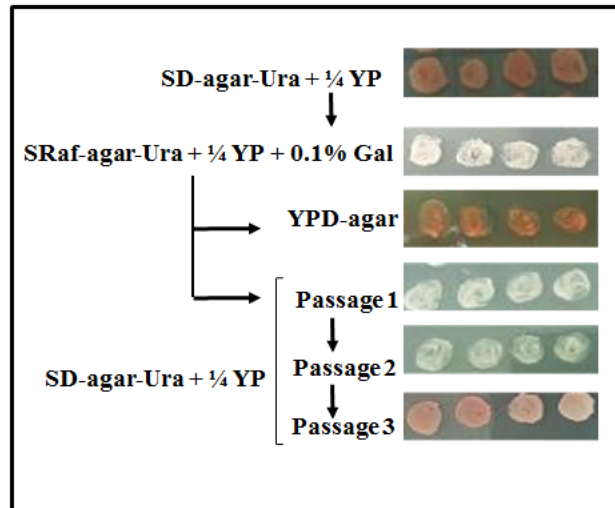the 64-D yeast with *erg6Δ* mutation also lead to red to white color switch (**Figure 16**).

Figure 16: Red to white color switch in *erg6Δ ade1-14* yeast

Furthermore, the color switch was also reversible and dependent on the sustained expression of the amyloid similar to the observations in the 74-D-694 background thereby validating the amyloid-induced red to white color switch model in the *erg6Δ ade1-14* yeast (**Figure 16**).

Chapter 4

Conclusion

In this work, amyloid proteins TDP-43-YFP, Aβ-42-GFP or Poly-Q$_{103}$-GFP inducing oxidative stress in yeast models of Amyotrophic Lateral sclerosis (ALS), Alzheimer's and Huntington's was studied. Oxidative stress caused by the amyloids was correlated with the phenotypic color switch in *ade1-14* and *erg6Δ ade1-14* double mutant yeast. The observed phenotypic change was reversible if the expression of amyloid proteins in yeast was stopped. Also, this colour change was reversed by reducing the oxidative stress by providing reducing environment to yeast cell with reducing agents such as ascorbic acid. Mitochondrial damage was assessed by the amount of dehydrogenase present in the yeast cells expressing TDP-43 using TTC assay and it was found that even though there is no significant number of petites (yeast cells without functional mitochondria), amyloid induced mitochondrial damage is observed in yeast system. From these observations, we correlated the white colonies in *ade1-14* yeast after the expression of amyloid proteins to be a marker of protein aggregation and oxidative stress caused by amyloids. The observation that this color assay can respond to any oxidative stress-inducing amyloid, can make it a general and versatile tool for anti-amyloid and anti-oxidative stress drug screening in the yeast model.

References

[1] Leopold, P.E., M. Montal, and J.N. Onuchic, Protein folding funnels: a kinetic approach to the sequence-structure relationship. Proc Natl Acad Sci U S A, 1992. **89**(18): p. 8721-5.

[2] Jahn, T.R. and S.E. Radford, The Yin and Yang of protein folding. FEBS J, 2005. **272**(23): p. 5962-70.

[3] Herczenik, E. and M.F. Gebbink, Molecular and cellular aspects of protein misfolding and disease. FASEB J, 2008. **22**(7): p. 2115-33.

[4] Rambaran, R.N. and L.C. Serpell, Amyloid fibrils: abnormal protein assembly. Prion, 2008. **2**(3): p. 112-7.

[5] Chiti, F. and C.M. Dobson, Protein misfolding, functional amyloid, and human disease. Annu Rev Biochem, 2006. **75**: p. 333-66.

[6] Biancalana, M. and S. Koide, Molecular mechanism of Thioflavin-T binding to amyloid fibrils. Biochim Biophys Acta, 2010. **1804**(7): p. 1405-12.

[7] Nelson, R., et al., Structure of the cross-beta spine of amyloid-like fibrils. Nature, 2005. **435**(7043): p. 773-8.

[8] Patel, B.K. and S.W. Liebman, "Prion-proof" for [PIN+]: infection with in vitro-made amyloid aggregates of Rnq1p-(132-405) induces [PIN+]. J Mol Biol, 2007. **365**(3): p. 773-82.

[9] Liebman, S.W. and Y.O. Chernoff, Prions in yeast. Genetics, 2012. **191**(4): p. 1041-72.

[10] Prusiner, S.B., Prions. Proc Natl Acad Sci U S A, 1998. **95**(23): p. 13363-83.

[11] Summers, D.W. and D.M. Cyr, Use of yeast as a system to study amyloid toxicity. Methods, 2011. **53**(3): p. 226-31.

[12] Pereira, C., et al., Contribution of yeast models to neurodegeneration research. J Biomed Biotechnol, 2012. **2012**: p. 941232.

[13] Khurana, V. and S. Lindquist, Modelling neurodegeneration in Saccharomyces cerevisiae: why cook with baker's yeast? Nat Rev Neurosci, 2010. **11**(6): p. 436-49.

[14] Wickner, R.B., [URE3] as an altered URE2 protein: evidence for a prion analog in Saccharomyces cerevisiae. Science, 1994. **264**(5158): p. 566-569.

[15] Chernoff, Y.O., The call of the unknown: The story of [PSI(+)]. Prion, 2015. **9**(5): p. 315-7.

[16] Tuite, M.F., G.L. Staniforth, and B.S. Cox, [PSI(+)] turns 50. Prion, 2015. **9**(5): p. 318-32.

[17] Figley, M.D. and A.D. Gitler, Yeast genetic screen reveals novel therapeutic strategy for ALS. Rare Dis, 2013. **1**: p. e24420.

[18] Park, S.K., et al., Development and validation of a yeast high-throughput screen for inhibitors of Abeta(4)(2) oligomerization. Dis Model Mech, 2011. **4**(6): p. 822-31.

[19] Manogaran, A.L., et al., Prion Formation and Polyglutamine Aggregation Are Controlled by Two Classes of Genes. PLoS Genet, 2011. **7**(5): p. e1001386.

[20] Cox, B., PSI, a cytoplasmic suppressor of super-suppressor in yeast. Heredity, 1965. **20**(121): p. 505-521.

[21] Hong, J.Y., V. Mathur, and S.W. Liebman, A new colour assay for [URE3] prion in a genetic background used to score for the [PSI(+)] prion. Yeast, 2011. **28**(7): p. 555-60.

[22] Burns, A. and S. Iliffe, Alzheimer's disease. BMJ, 2009. **338**.

[23] Pescosolido N, P.A., Buomprisco G, Rusciano D, Critical Review on the Relationship between Glaucoma and Alzheimer's Disease. Adv Ophthalmol Vis Syst, 2014. **1**(4).

[24] Huang, Y. and L. Mucke, Alzheimer mechanisms and therapeutic strategies. Cell, 2012. **148**(6): p. 1204-22.

[25] Bayer, T.A., et al., It all sticks together--the APP-related family of proteins and Alzheimer's disease. Mol Psychiatry, 1999. **4**(6): p. 524-8.

[26] Palop, J.J. and L. Mucke, Amyloid-β Induced Neuronal Dysfunction in Alzheimer's Disease: From Synapses toward Neural Networks. Nature neuroscience, 2010. **13**(7): p. 812-818.

[27] Palop, J.J. and L. Mucke, Epilepsy and Cognitive Impairments in Alzheimer Disease. Arch Neurol, 2009. **66**(4): p. 435.

[28] Verret, L., et al., Inhibitory Interneuron Deficit Links Altered Network Activity and Cognitive Dysfunction in Alzheimer Model. Cell, 2012. **149**(3): p. 708-721.

[29] Cummings, J.L., Alzheimer's Disease. New England Journal of Medicine, 2004. **351**(1): p. 56-67.

[30] Citron, M., Alzheimer's disease: strategies for disease modification. Nat Rev Drug Discov, 2010. **9**(5): p. 387-398.

[31] Schor, N.F., What the halted phase III γ-secretase inhibitor trial may (or may not) be telling us. Ann Neurol, 2011. **69**(2): p. 237-239.

[32] Schirmer, R.H., et al. Lest we forget you methylene blue Neurobiol Aging. **32**(12): p. 2325.e7-2325.e16.

[33] Gura, T., Hope in Alzheimer's fight emerges from unexpected places. Nat Med, 2008. **14**(9): p. 894-894.

[34] Kim, J., et al., Haploinsufficiency of human APOE reduces amyloid deposition in a mouse model of Aβ amyloidosis. The Journal of Neuroscience, 2011. **31**(49): p. 18007-18012.

[35] Bagriantsev, S. and S. Liebman, Modulation of Abeta42 low-n oligomerization using a novel yeast reporter system. BMC Biol, 2006. **4**: p. 32.

[36] Chen, X. and D. Petranovic, Amyloid-beta peptide-induced cytotoxicity and mitochondrial dysfunction in yeast. FEMS Yeast Res, 2015. **15**(6).

[37] Gillian P. Bates, R.D., James F. Gusella, Michael R. Hayden, Chris Kay, Blair R. Leavitt, Martha Nance, Christopher A. Ross, Rachael I. Scahill, Ronald Wetzel, Edward J. Wild & Sarah J. Tabrizi, Huntington disease. Nature Reviews Disease Primers, 2015. **1**: p. 15052.

[38] Meriin, A.B., et al., Huntington toxicity in yeast model depends on polyglutamine aggregation mediated by a prion-like protein Rnq1. J Cell Biol, 2002. **157**(6): p. 997-1004.

[39] Duennwald, M.L., et al., A network of protein interactions determines polyglutamine toxicity. Proc Natl Acad Sci U S A, 2006. **103**(29): p. 11051-6.

[40] Derkatch, I.L., et al., Effects of Q/N-rich, polyQ, and non-polyQ amyloids on the de novo formation of the [PSI+] prion in yeast and aggregation of Sup35 in vitro. Proc Natl Acad Sci U S A, 2004. **101**(35): p. 12934-9.

[41] Solans, A., et al., Cytotoxicity of a mutant huntingtin fragment in yeast involves early alterations in mitochondrial OXPHOS complexes II and III. Hum Mol Genet, 2006. **15**(20): p. 3063-81.

[42] Ehrnhoefer, D.E., et al., Green tea (-)-epigallocatechin-gallate modulates early events in huntingtin misfolding and reduces toxicity in Huntington's disease models. Hum Mol Genet, 2006. **15**(18): p. 2743-51.

[43] Zhang, X., et al., A potent small molecule inhibits polyglutamine aggregation in Huntington's disease neurons and suppresses neurodegeneration in vivo. Proc Natl Acad Sci U S A, 2005. **102**(3): p. 892-7.

[44] Bodner, R.A., et al., Pharmacological promotion of inclusion formation: a therapeutic approach for Huntington's and Parkinson's diseases. Proc Natl Acad Sci U S A, 2006. **103**(11): p. 4246-51.

[45] Sarkar, S., et al., Small molecules enhance autophagy and reduce toxicity in Huntington's disease models. Nat Chem Biol, 2007. **3**(6): p. 331-8.

[46] Johnson, B.S., et al., TDP-43 is intrinsically aggregation-prone, and amyotrophic lateral sclerosis-linked mutations accelerate aggregation and increase toxicity. J Biol Chem, 2009. **284**(30): p. 20329-39.

[47] Lee, E.B., V.M.Y. Lee, and J.Q. Trojanowski, Gains or losses: molecular mechanisms of TDP43-mediated neurodegeneration. Nat Rev Neurosci, 2011. **13**(1): p. 38-50.

[48] Scotter, E.L., H.J. Chen, and C.E. Shaw, TDP-43 Proteinopathy and ALS: Insights into Disease Mechanisms and Therapeutic Targets. Neurotherapeutics, 2015. **12**(2): p. 352-63.

[49] Saccon, R.A., et al., Is SOD1 loss of function involved in amyotrophic lateral sclerosis? Brain, 2013. **136**(Pt 8): p. 2342-58.

[50] Rossi, S., M. Cozzolino, and M.T. Carri, Old versus New Mechanisms in the Pathogenesis of ALS. Brain Pathol, 2016. **26**(2): p. 276-86.

[51] Wang, I.F., et al., Autophagy activators rescue and alleviate pathogenesis of a mouse model with proteinopathies of the TAR DNA-binding protein 43. Proc Natl Acad Sci U S A, 2012. **109**(37): p. 15024-15029.

[52] Kim, H.-J., et al., Therapeutic modulation of eIF2α-phosphorylation rescues TDP-43 toxicity in amyotrophic lateral sclerosis disease models. Nature genetics, 2014. **46**(2): p. 152-160.

[53] Lee, B.-H., et al., Enhancement of Proteasome Activity by a Small-Molecule Inhibitor of Usp14. Nature, 2010. **467**(7312): p. 179-184.

[54] van Langenhove, T., J. van der Zee, and C. van Broeckhoven, The molecular basis of the frontotemporal lobar degeneration–amyotrophic lateral sclerosis spectrum. Annals of Medicine, 2012. **44**(8): p. 817-828.

[55] Fushimi, K., et al., Expression of human FUS/TLS in yeast leads to protein aggregation and cytotoxicity, recapitulating key features of FUS proteinopathy. Protein Cell, 2011. **2**(2): p. 141-9.

[56] Braun, R.J., Mitochondrion-mediated cell death: dissecting yeast apoptosis for a better understanding of neurodegeneration. Front Oncol, 2012. **2**: p. 182.

[57] Sharma, K.G., R. Kaur, and A.K. Bachhawat, The glutathione-mediated detoxification pathway in yeast: an analysis using the red pigment that accumulates in certain adenine biosynthetic mutants of yeasts reveals the involvement of novel genes. Arch Microbiol, 2003. **180**(2): p. 108-17.

[58] Sharma, K.G., et al., Localization, regulation, and substrate transport properties of Bpt1p, a Saccharomyces cerevisiae MRP-type ABC transporter. Eukaryot Cell, 2002. **1**(3): p. 391-400.

[59] Derkatch, I.L., et al., Genesis and variability of [PSI] prion factors in Saccharomyces cerevisiae. Genetics, 1996. **144**(4): p. 1375-86.

[60] Sikorski, R.S. and P. Hieter, A system of shuttle vectors and yeast host strains designed for efficient manipulation of DNA in Saccharomyces cerevisiae. Genetics, 1989. **122**(1): p. 19-27.

[61] Sherman, F., Fink, G. R. & Hicks, J. B., Methods in Yeast Genetics Cold Spring Harbor Laboratory Press, Cold Spring Harbor, NY, 1986.

[62] Schneider, C.A., W.S. Rasband, and K.W. Eliceiri, NIH Image to ImageJ: 25 years of image analysis. Nat Meth, 2012. **9**(7): p. 671-675.

[63] T. J. Burdock, M.S.B.a.A.E.G., A Dehydrogenase Activity Test for Monitoring the Growth of Streptomyces Venezuelae in a Nutrient Rich Medium. J Bioprocess Biotechniq, 2011. **1**.

[64] Kozo Ouchi, H.S., Masahiko Shimoda, Hiroichi Akiyama & Takamichi Nishiya, Isolation of Uracil Auxotrophic Mutants of Saccharomyces cerevisiae Unable to Reduce 2,3,5-Triphenyl-tetrazolium Chloride. Agricultural and Biological Chemistry, 1984.

[65] Vallieres, C., et al., A rapid in vivo colorimetric library screen for inhibitors of microbial respiration. ACS Chem Biol, 2012. **7**(10): p. 1659-65.

[66] Doronina, V.A., et al., Oxidative stress conditions increase the frequency of de novo formation of the yeast [PSI+] prion. Mol Microbiol, 2015. **96**(1): p. 163-74.

[67] D'Angelo, F., et al., A yeast model for amyloid-beta aggregation exemplifies the role of membrane trafficking and PICALM in cytotoxicity. Dis Model Mech, 2013. **6**(1): p. 206-16.

[68] Sherman, M.Y. and P.J. Muchowski, Making yeast tremble: yeast models as tools to study neurodegenerative disorders. Neuromolecular Med, 2003. **4**(1-2): p. 133-46.

[69] M. Ogur, R.S.J.a.S.N., Tetrazolium overlay technique for population studies of respiration deficiency in yeast. science, 1957.

[70] Welihinda, A.A., A.D. Beavis, and R.J. Trumbly, Mutations in LIS1 (ERG6) gene confer increased sodium and lithium uptake in Saccharomyces cerevisiae. Biochim Biophys Acta, 1994. **1193**(1): p. 107-17.

[71] Longtine, M.S., et al., Additional modules for versatile and economical PCR-based gene deletion and modification in Saccharomyces cerevisiae. Yeast, 1998. **14**(10): p. 953-61.